# *WT3 Generic Models for Transient Stability Studies of Wind Turbine Generators*

Diogo Eiró, under supervision of J. M. Ferreira de Jesus

***Abstract*—Given the increasing penetration of wind energy in the power system, not only at a national, but also global level, the need for the scientific and academic community to better understand this technology is rapidly growing. For that purpose, the effort of several international entities has greatly contributed, with the creation of generic models capable of accurately representing the multitude of wind turbine generators, WTGs, available in the present-day market. These models can be of type 1, 2, 3 or 4 (A, B, C or D in some literature), depending on the generator's topology and grid interface.**

**This article focuses on the type 3 generic model, WT3, which represents a WTG composed of a doubly-fed induction generator, DFIG, equipped with an AC/DC/AC power converter connecting the rotor to the grid and the stator directly connected to the grid. This being the most used technology nowadays.**

**The work was developed in MATLAB based on an academic program for dynamic simulations of electric power systems for transient stability studies that has been developed throughout the years by IST students.**

**With the goal of implementing type 3 generic models in this program, it was firstly necessary to understand the program itself, then, the type 3 wind generator and its generic model were studied at length to then be implemented, in a final stage of this work. Finally, several simulations were run and the results obtained were validated against results obtained with the PSS/E™ software.**

***Keywords:*** **Wind Energy, WTG, Generic Models, Transient Stability, PSS/E™**

## I. INTRODUCTION

Successive technological advances and a growing global concern about sustainability and energy efficiency have contributed to the use of renewable energy sources (RES) becoming increasingly unavoidable today. Their "clean" form of energy production, helping governments meet ever more stringent environmental targets and increasing their market competitiveness, has made their use viable.

In view of the environmental targets set for each country, more and more countries are investing in RES, with wind energy being given great attention. Portugal is an example of this. In 2015, it was the fourth country in the European Union with the greatest incorporation of renewable energies in electricity generation. This position was mainly due to the contribution of water and wind energy sources, which accounted for 84% of RES according to (DGEG, 2016).

In 2016, according to technical data provided by (REN, 2016), RES represented 57% of national consumption, which compared with 47% in the previous year, clearly shows the effort that has been made in our country.

To this end, the continued growth of wind technology since the year 2000 has been a key factor in the national strategic focus on endogenous and renewable resources for the diversification of sources, improved security of supply, reduction of energy dependence and reduction of the impact of the electroproduction system on the environment. Thus, almost two decades later, wind energy as became an indispensable resource in the national electric mix, and, according to DGEG, the technology that, between 2007 and 2016, presented the greatest increase in installed power, in the amount of 2.8 GW, reaching a total of 5322 MW.

In terms of electricity production, in 2016 wind farms generated 12,188 GWh, representing 22% of national production and 40% of renewable production.

In view of this growing and already considerable penetration of wind energy, the need to better understand its behavior both in steady and transient state in the occurrence of faults in the network has greatly increased. With this in mind, a great effort has been made by several entities in the creation of generic models of wind generators. These models have been included in several commercial power simulation tools such as the PSS/E™ software, which is one of the most widely used tools today.

It is in this context that the motivation for this work arises. Over the years, several IST students (Paulo, 2008), (Araújo, 2009) and (Lacerda, 2013) have been developing, in MATLAB, a program for dynamic simulations of electrical energy systems for transient stability studies. The work of this dissertation will focus on the expansion of the library of models of this same program, through the inclusion of WTG generic models.

The model to be implemented is the generic model of a WTG consisting of a DFIG known in the literature as WT3. This would be because this is the dominant topology in the market today, according to (Ferreira de Jesus & Castro, 2004) and (Cheng, 2015, p. 30)

This model was taken from PSS/E™ library of models, and is composed of the following four sub models:

Table 1 – Dynamic Models Implemented and PSS/E™ nomenclature

| Dynamic Model | Nomenclature |
|---|---|
| Wind turbine generator/converter model | WT3G1 |
| Wind turbine electrical control model | WT3E1 |
| Wind turbine mechanical control model | WT3T1 |
| Wind turbine *pitch* control model | WT3P1 |

After the study and implementation of the generic WT3 model in the program, several simulations were run and their results compared with PSS/E™ results to validate the work developed.

The paper is organized as follows: Section II describes the developed simulation software, in Section III the generic WT3 model is presented, in Section IV the model's differential representation is given, the model validation is shown in Section V and finally, section VI presents the conclusions of this work.

## II. POWER SYSTEMS SIMULATION SOFTWARE

The simulation process is divided into five main routines.

### *A. Simulation Data Acquisition*

In this first stage, the data files are read. The data for the simulation is contained in two separate files: the *.raw file, which contains the information regarding the network, and the

*.dyr, which holds all the information regarding the dynamic models.

### *B. Power Flow Computation*

The initial power flow is computed in this step using the well-known Newton-Raphson method. Its results will then be used to convert loads and generators and to compute the initial conditions required for dynamic simulation.

### *C. Preliminary Calculations*

Before the start of the dynamic simulation, the necessary preliminary calculations are performed.
First, the admittance matrix, $[Y]$, is computed considering all the loads properly converted to constant admittances and the generators represented by their equivalent impedance. This matrix is then reduced, using the method presented in (Sucena Paiva, 2005), and the $[\boldsymbol{Y}_{aux}]$ is computed. This matrix will be used in the calculation of voltages in all buses of the network.
Next, the initial condition for all the variables involved is calculated.
Finally, the constant matrices for the algebraic state equations, used in the digital numerical integration, are calculated.

### *D. Dynamic Simulation*

The simulation is performed in several small step times. In each step time, a new set of solutions for the variables is computed.
The simulation begins at $t = 0(s)$. The first action to take place is the verification that there are no changes in $[Y]$, when there are it means that a fault has occurred and so the network matrix must be recalculated.
After this, the model's algebraic variables are computed. These variables will be the voltages $\boldsymbol{V}$ of each bus and the injected currents of each generator, $\boldsymbol{I}_{inj}$. The generator's internal voltage $\boldsymbol{E}$ is given by (1) where $\boldsymbol{I}_{sorc}$ is current value of the generator's Norton equivalent. The voltage matrix $\boldsymbol{V}$ is then computed using (2), finally the injected current is given by (3), where $\boldsymbol{V}_{term} = \boldsymbol{V}_i$, here, i indicates the bus where the generator is connected.

$$\boldsymbol{E} = \boldsymbol{I}_{sorc}.\boldsymbol{X}_{eq} \tag{1}$$

$$\boldsymbol{V} = \boldsymbol{Y}_{aux}.\boldsymbol{E} \tag{2}$$

$$[\boldsymbol{I}_{inj}] = \boldsymbol{I}_{sorc} - \boldsymbol{V}_{term}.\boldsymbol{X}_{eq}{}^{-1} \tag{3}$$

Then, the complex power is obtained with (4), and consequently the generator's active and reactive powers are computed using (5) and (6).

$$\boldsymbol{S}_i = \boldsymbol{V}_i \boldsymbol{I}^*_{inj_i} \tag{4}$$

$$P_{G_i} = real\{\boldsymbol{S}_{maq_i}\} \tag{5}$$

$$Q_{G_i} = imag\{\boldsymbol{S}_{maq_i}\} \tag{6}$$

After this, the non-constant matrices for the algebraic state equations are computed and finally, the numeric integration algorithm is performed resulting in new values for each state variable that must be checked to see if they respect the limits imposed by the model. As in the previous versions, the integration algorithm used was the modified Euler-Cauchy method. Time is then incremented by one time-step, and if the maximum time is not reached, the simulation repeats the cycle.

### *E. Printing Results*

Once the maximum time is reached, the results are plotted and the program ends.

## III. GENERIC WT3 MODEL

### *F. Aerodynamics*

Modern WTGs generate electricity by converting the energy contained in the wind.
The total available power, $P_v$ [W], contained in a volume of air that passes through the area of the WTG blades, A $[m^2]$, at a speed v $[m/s]$ is:

$$P_v = \frac{1}{2}\rho_{ar} A v^3 \tag{7}$$

The fraction of power extracted from the power in the wind by a WTG is usually given by the symbol $C_p$, standing for the coefficient of performance or power coefficient. Using this notation, the actual mechanical power output of a WTG can be written as:

$$P_m = \frac{1}{2}\rho_{ar} C_p A v^3 \tag{8}$$

The value of $C_p$ depends on tip speed ratio, $\lambda$, and blade pitch angle, β, based on the turbine characteristics as follows:

$$C_p = C_1\left(\frac{C_2}{\lambda_i} - C_3\beta - C_3\beta^{C_5} - C_6\right) e^{\left(-\frac{C_7}{\lambda_i}\right)} \tag{9}$$

$$\lambda = \frac{\omega_t R}{v} \tag{10}$$

$$\lambda_i = \frac{1}{\frac{1}{\lambda - C_8\beta} - \frac{C_9}{\beta^3 + 1}} \tag{11}$$

where $C_1$ to $C_6$ denote characteristic coefficients of WTGs and $\omega_t$ $[rad/s]$ is the rotational speed of turbine and $\omega_t$ $[rad/s]$. The $C_p$ characteristics for different values of β is shown in `Fig. 1`:

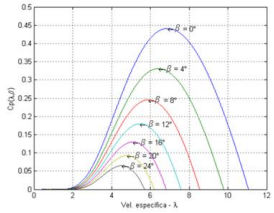

Fig. 1. - $C_p$ characteristics

### *G. Mechanical Model*

The drive train of a WTG generator system consists of a blade-pitching mechanism with a spinner, a hub with blades, a rotor shaft and a gearbox with breaker and generator. Depending on the complexity of the study, the complexity of the drive train modeling differs. For example, when problems such as torsional fatigue are studied, dynamics of all parts must be considered. For these reasons, two-lumped mass or more sophisticated models are required. Fig. 2 shows the two-lumped mass model:

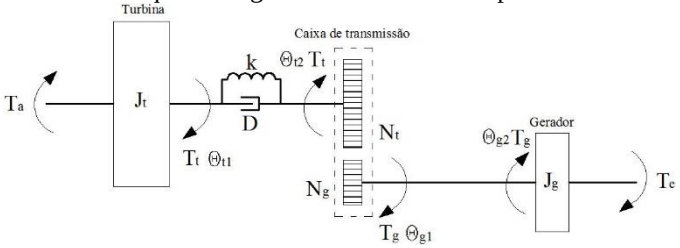


Fig. 2. - two-lumped mass model

The model is defined by the following equations:

$$2H_t \frac{d\omega_t(t)}{dt} = T_a - k\left(\theta_{t1}(t) - \theta_{g2}(t)\right) - D\left(\omega_t(t) - \omega_g(t)\right) \quad (12)$$

$$2H_g \frac{d\omega_g(t)}{dt} = -T_e + k\left(\theta_{t1}(t) - \theta_{g2}(t)\right) + D\left(\omega_t(t) - \omega_g(t)\right) \quad (13)$$

$$\frac{d\left(\theta_{t1} - \theta_{g2}\right)}{dt} = \omega_t(t) - \omega_g(t) \quad (14)$$

Where $T_a\ [Nm]$ is the mechanical torque of the WTG, $K\ [Nm/rad]$ is the spring constant, $D$ is the damping coefficient $[Nms/rad]$, $\omega_g\ [rad/s]$ is the mechanical angular speed of the generator, $T_e\ [Nm]$, is the electromechanical torque, and $H_t$ and $H_g\ [s]$ are the inertia constants of the turbine and the generator.

However, when the study focuses on the interaction between wind farms and grid system, the drive train can be treated as one-lumped mass model with acceptable precision for the sake of time efficiency. The model is defined by equation (14):

$$22\left(H_t + H_g\right)\frac{d\omega_g(t)}{dt} = T_a - T_e \quad (15)$$

*H. Generator*

Despite the seemingly large variety of utility-scale WTGs in the market, each can be classified in one of four basic types described below. The classification is based on the type of generator and grid interface, as shown in Figure 3.

- Type-1 – Fixed-speed, induction generator
- Type-2 – Variable slip, induction generators with variable rotor resistance
- Type-3 – Variable speed, doubly-fed asynchronous generators with rotor-side converter
- Type-4 – Variable speed generators with full converter interface

As indicated, the type 3 model is the focus of this work. Wind generators of this type are composed by a doubly fed induction generator, DFIG. This is a wound rotor induction machine that is connected so that it allows the transfer of active power through both the rotor and stator windings. The rotor winding is connected to the grid via a power electronic frequency converter with a rating of about 30 % of the total power rating of the WTG. In normal operation the active and reactive power of the turbine can be controlled quickly and independently by the converter

The WT3 model, provided in PSSE's library and used in this work, is a simplified generic model intended for bulk power system studies where a detailed representation of a WTG is not required.

The modelling of WT3 for load flow analysis is generally simple. Wind plants normally consist of many individual WTGs. While the Wind Plant model may consist of a detailed representation of each WTG and the collector system, a simpler model is appropriate for most bulk system studies. Such a model can be shown in Fig. 3.


Fig. 3 - Simplified Power Flow model (Muljadi & Elis, 2009)

The complete WTG is divided into four functional sub models, as indicated in Fig. 4.

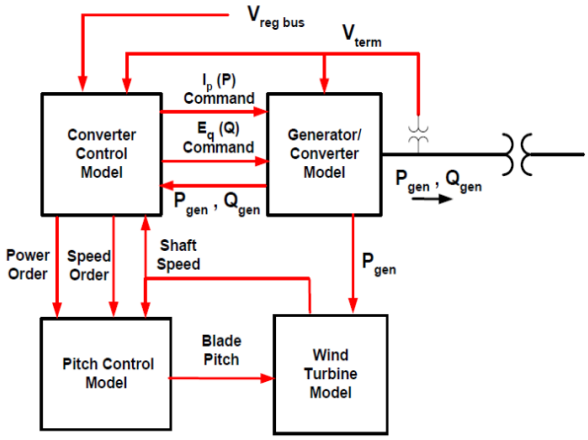


Fig. 4. - WT3 model connectivity diagram (Siemens, 2015).

In the next section, a brief description of these models is given and the differential equations are computed. In the dynamic simulation, where these equations are used, the windup and anti-windup limits will play an essential role. These limits maintain the system within boundaries to avoid possible damage. These limits are thoroughly documented in (Milano, 2010).

## IV. DIFFERENTIAL-ALGEBRAIC MODELS

*I. WT3G1 model*

Fig. 5 shows the generator/converter model. The output of the model is a controlled current source that computes the required injected current into the network in response to the flux and active current commands from the electrical control model. The converter control includes a phase-locked loop to synchronize the generator rotor currents with the stator. The function of the converter phase-locked loop is to establish a reference frame for the WTG voltages and currents, which is shown in the phase diagram in Fig. 6.

In steady-state $V_X = V_{term}$. In the event of a system disturbance, the rate of change is limited by the PLL logic. $X_{eq}$ represents an equivalent reactance of the generator effective reactance.

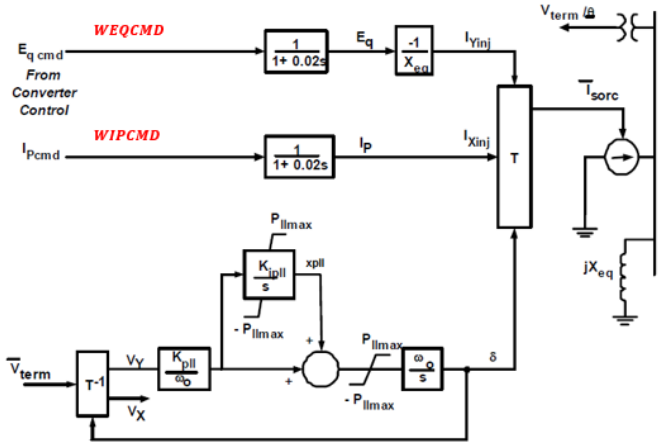


Fig. 5 - Generator/Converter model, WT3G1 (Siemens, 2015)

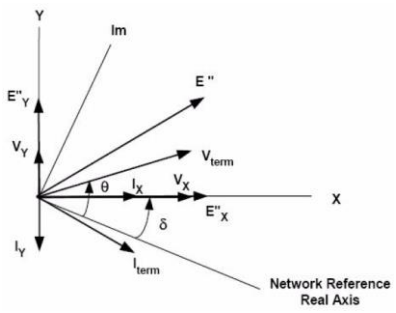


Fig. 6 - Phase diagram of the voltages and currents (Siemens, 2015)

The differential state equations that represent the WT3G1 model are:

$$\frac{dI_p}{dt} = \frac{1}{0{,}02}.\left(WIPCMD - I_p\right) \tag{16}$$

$$\frac{dE_q}{dt} = \frac{1}{0{,}02}.\left(WEQCMD - E_q\right) \tag{17}$$

$$\frac{dx_{pll}}{dt} = \frac{K_{pll}.K_{ipll}.V_Y}{\omega_s} \tag{18}$$

$$\frac{d\delta}{dt} = \omega_s.\left(x_{pll} + \frac{K_{pll}}{\omega_s}.V_y\right) \tag{19}$$

*J. WT3E1 model*

Fig. 7 shows the electrical control model. This model dictates the active and reactive power to be delivered to the system.

In the reactive power control branch (Fig.5 top) the switch, VARFLG, provides for 3 modes of control:

constant reactive power, constant power factor angle, or voltage regulation by a wind plant reactive power controller. The switch, VLTFLG, provides for bypassing the closed loop terminal voltage regulator, which is not used in all implementations.

The compensated voltage, $V_C$ input to the wind plant reactive power control emulator is calculated as $V_C = V_{reg} - jX_C.I_{reg}$ = where $V_{reg}$ is complex voltage at "regbus", $I_{reg}$ complex current measured in branch from "regbus" to "tobus".

In the active power control branch (Fig.5 bottom) system. The non-linear function, f($P_{elec}$), is used to model the desired generator's speed as a function of the power level. The input data for this function are values of the desired speed at specific levels of active power. The output of the function is found using linear interpolation. In appendix A default parameters given in (Siemens, 2015) are provided and a typical Power vs Speed characteristic is shown.

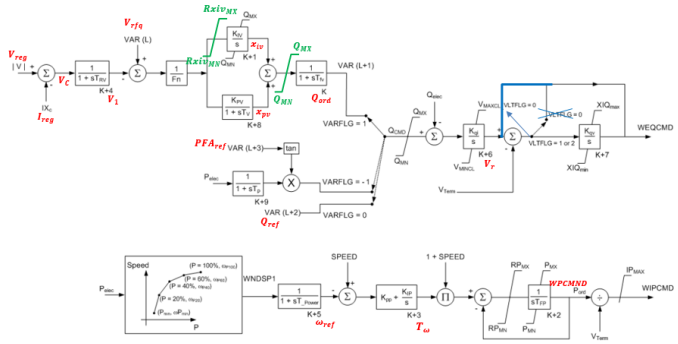

Fig. 7 - Electrical control model, WT3E1 (Siemens, 2015)

The differential state equations that represent the WT3E1 model are:

$$\frac{dWPCMND}{dt} = \frac{1}{T_{fp}}\left[\left(T_\omega + K_{pp}.\left(SPEED - \omega_{ref}\right)\right).(1 + SPEED) - WPCMND\right] \tag{20}$$

$$\frac{dT_\omega}{dt} = K_{ip}.\left(SPEED - \omega_{ref}\right) \tag{21}$$

$$\frac{d\omega_{ref}}{dt} = \frac{1}{T_{power}}(WNDSP1 - \omega_{ref}) \tag{22}$$

$$\frac{dV_r}{dt} = K_{qi}.(Q_{cmd} - Q_{elec}) \tag{23}$$

If $VARFLG = 1$:

$$\frac{dQ_{ord}}{dt} = \frac{1}{T_{fv}}(xiv + xpv - Q_{ord}) \tag{24}$$

$$\frac{dx_{iv}}{dt} = \frac{K_{iv}}{F_n}(V_{rfq} - V_1) \tag{25}$$

$$\frac{dx_{Pv}}{dt} = \frac{1}{T_v}\left[(V_{rfq} - V_1).\frac{K_{pv}}{F_n} - x_{Pv}\right] \tag{26}$$

$$\frac{dV_1}{dt} = \frac{1}{T_{rv}}(V_C - V_1) \tag{27}$$

If $VARFLG = -1$

$$\frac{dPFA}{dt} = \frac{1}{T_p}(P_{elec} - PFA) \tag{28}$$

If $VLTFLG = -1$:

$$\frac{dWEQCMD}{dt} = K_{qv}.(V_r - V_{term}) \tag{29}$$

*K. WT3T1 model*

The mechanical system model is shown in Fig. 8 for its two-lumped mass representation and in Fig. 9 for its simplified single mass representation. The first part of this model, the simplified aerodynamic model, receives the desired pitch from the pitch control model and calculates the mechanical power, the second part, which models the shaft dynamics, then computes the desired speed deviation required to extract the maximum amount of power from the wind.

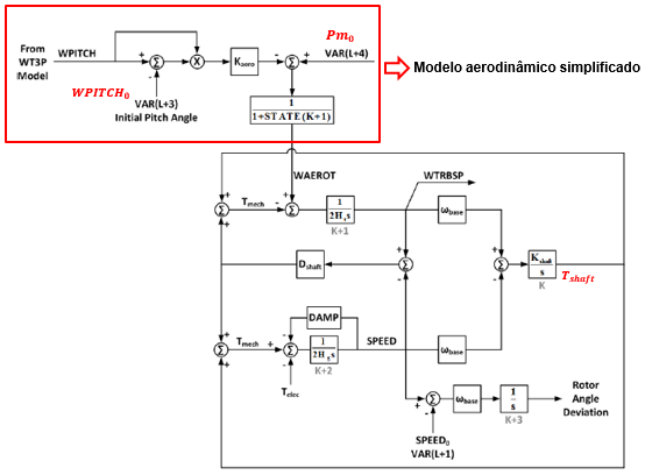


Fig. 8 – Two-lumped Mass Mechanical Control model, WT3T1 (Siemens, 2015)

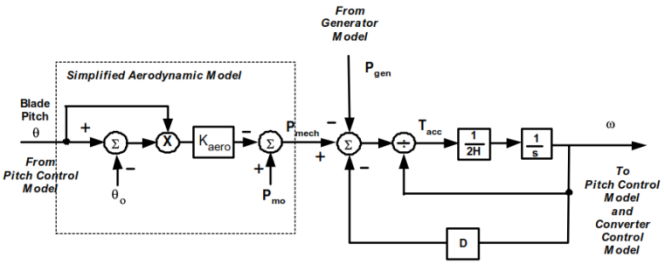


Fig. 9 - Single Mass Mechanical Control model, WT3T1 (Yuriy & Krishnat, 2009)

The differential state equations that represent the two-lumped mass model of the WT3T1 are:

$$\frac{dSPEED}{dt} = \frac{1}{2H_g}.\left(T_{shaft} + (WTRBSP - SPEED).D_{shaft} - T_{elec} - SPEED.DAMP\right) \quad \text{(III.30)}$$

$$\frac{dWTRBSP}{dt} = \frac{1}{2H_t}.\left(WAEROT - T_{shaft} - (WTRBSP - SPEED).D_{shaft}\right) \quad \text{(III.31)}$$

$$\frac{dT_{shaft}}{dt} = K_{shaft}.\omega_{base}(WTRBSP - SPEED) \quad \text{(III.32)}$$

Where:

$$WAEROT = \frac{Pmo - K_{aero}.(WPITCH - WPITCH_0).WPITCH}{1 + WTRBSP} \quad \text{(III.33)}$$

$$T_{elec} = \frac{P_{elec}}{1 + SPEED} \quad \text{(III.34)}$$

As for the single mass model of the WT3T1, the differential state equation is:

$$\frac{dSPEED}{dt} = \frac{1}{2H}.(WAEROT - T_{elec} - SPEED.DAMP) \quad \text{(III.35)}$$

Where:

$$WAEROT = \frac{Pmo - K_{aero}.(WPITCH - WPITCH_0).WPITCH}{1 + SPEED} \quad \text{(III.36)}$$

*L. WT3P1 model*

The pitch control model, shown in Fig. 10, controls the mechanical system and its main purpose is to assure the maximum extraction of mechanical power from the available wind, without exceeding the generator's nominal power. It is composed of two PI controllers, the pitch control and the pitch compensation. For wind speeds below the rotor's nominal speed, the pitch is maintained at its minimum value, 0º, to maximize the power extraction. For wind speeds above the rotor's nominal speed the pitch is increased gradually to reduce the speed reached by the generator's rotor thereby limiting the mechanical power.

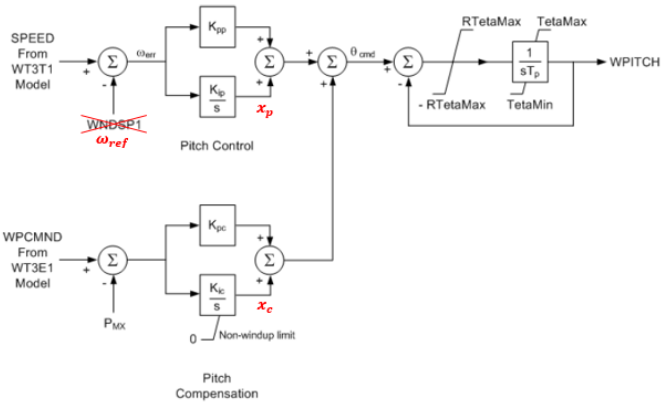


Fig. 10 - Pitch Control model, WT3P1 (Siemens, 2015) [modified]

The differential state equations that represent the WT3P1 model are:

$$\frac{dWPITCH}{dt} = \frac{1}{T_p}.(\theta_{cmd} - WPITCH) \quad \text{(III.37)}$$

$$\frac{dx_p}{dt} = K_{ip}.\left(SPEED - \omega_{ref}\right) \quad \text{(III.38)}$$

$$\frac{dx_C}{dt} = K_{ic}.(WPCMND - P_{MX}) \quad \text{(III.39)}$$

Where:

$$\theta_{cmd} = x_p + K_{pp}.\left(SPEED - \omega_{ref}\right) + x_c + K_{pc}.(WPCMND - P_{MX}) \quad \text{(III.40)}$$

*M. Modifications in the WT3E1 and WT3P1 Models*

After several simulations were performed, it was concluded that the original models described in sections WT3E1 modelJ and L did not give a realistic transient behavior following a nearby three-phase short circuit.

An extensive troubleshoot and investigation were required to identify and solve the problem. The biggest differences occurred mainly in the WT3E1 model when the wind plant reactive power control was active (VARFLG = 1), when the closed loop terminal voltage regulator was bypassed (VLTFLG = 0) and in the pitch control regulator in the WT3P1 model.

The solution was the reparameterization of some values provided and recommended in PSS/E™ V34 for WT3E1, the implementation of two windup limits to limit the entrance values of the $x_{iv}$ and $Q_{ord}$ blocks of the reactive power control branch, the position of the flag VLTFLG was altered to also bypass the $V_{term}$ sum block and finally the WNDSP1 entrance at the WT3P1 model was replaced by the state variable $\omega_{ref}$. All these changes, properly indicated in Fig. 7 and Fig. 10, brought clear improvements in the model's response.

## V. Simulation Results

With the intent of validating the implemented dynamic models, a set of simulations were performed.

As noted in section J, the presence of the VARFLG and VLTFLG flags in the WT3E1 model allows for different types of control. Whether the value of VARFLG is set to -1, 0 or 1, the reactive power command, $Q_{cmd}$, will impose a constant power factor to the model, a constant reactive power or the control of the voltage in a bus chosen by the user. The value of

the VLTFLG flag can be set to 1 or 0, whether the generator's terminal voltage is to be controlled or not.
To access all the possible options for these flags, three simulations were performed with the following set of values:

- VARFLG = 1 and VLTFLG =1
- VARFLG = 0 and VLTFLG =1
- VARFLG = -1 and VLTFLG =0

The 5-bus network used in the simulations is presented in Fig. 11.

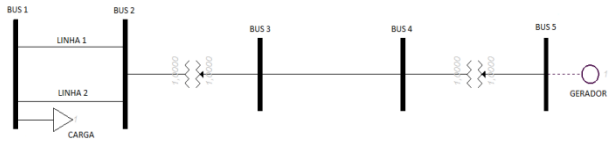


Fig. 11 - 5-bus network test system

All these simulations followed the same set of events:

- At $t = 0$ $[sec]$ the simulation starts;
- At $t = 1$ $[sec]$ a three-phase short circuit occurs on bus 1 of Fig. 11
- At $t = 1.15$ $[sec]$ the fault is cleared by the removal of branch 1.
- The simulation ends at $t = 20$ $[sec]$.

Also, all the simulations assume that the system base is 100 $[MVA]$, the nominal frequency is 50 $[Hz]$, and the time-step is $\Delta t = 0.001$ $[sec]$, which, as intended, is at least 4 smaller than the smallest time constant used.
For every simulation, even though the program offers the possibility of showing all the variables involved, only the most relevant ones are presented here. These will be the active and reactive powers, $P_{elec}$ and $Q_{elec}$, the generator's terminal voltage, $V_{term}$, the rotor's speed deviation, $SPEED$, the turbine blades' pitch angle, $WPITCH$, the aerodynamic torque $WAEROT$ and the current injected by the generator in the grid.
All the results obtained are presented hand in hand with their equivalents from the PSS/E™ software, represented by a yellow-highlighted area, to better compare and validate them.
The first step of the simulation is the initial power flow computation, the results obtained are given in Table 2, these will be valid for all simulations:

Table 2 – Power Flow Results

| *Bus* | *V* | *θ* | *Generation* | | *Load* | |
|---|---|---|---|---|---|---|
| | | | *P* | *Q* | *P* | *Q* |
| *1* | *0.9831* | *-8.78* | --- | --- | *50.00* | *5.00* |
| *2* | *0.9917* | *-5.11* | --- | --- | --- | --- |
| *3* | *0.9915* | *-2.18* | --- | --- | --- | --- |
| *4* | *0.9993* | *-1.45* | --- | --- | --- | --- |
| *5* | *1.000* | *0.00* | *50.71* | *2.00* | --- | --- |

*N. VARFLG = 1 and VLTFLG =1*

The results for this simulation are presented below:

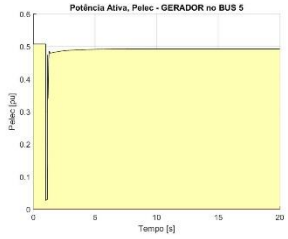


Fig. 12 - $P_{elec}$

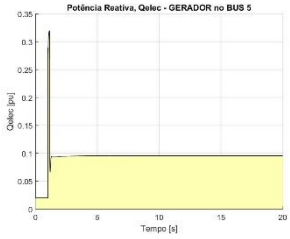


Fig. 13 - $Q_{elec}$

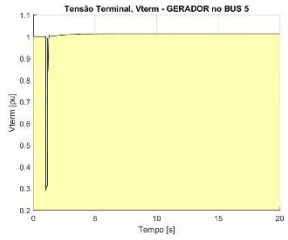


Fig. 14 - $V_{term}$

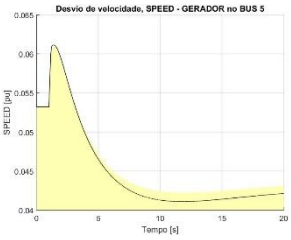


Fig. 15 – $SPEED$

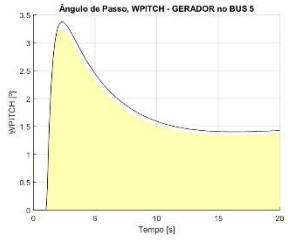


Fig. 16 - $WPITCH$

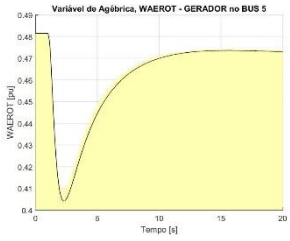


Fig. 17 – $WAEROT$

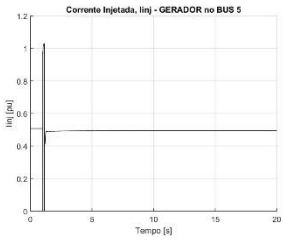


Fig. 18 – Injected Current

Before the fault, the system is in steady state, as can be seen from the figures above. This confirms that the initial conditions are correct. When the fault occurs, the generator's terminal voltage drops to near zero, as shown in Fig. 14, due to the presence of the low impedance characteristic of a short circuit. Consequently, there is a sudden increase in the current injected by the generator in the network, as shown in Fig. 18.
The active power presents a similar behavior to the terminal voltage, as is verified in Fig. 12. This decrease in the active power leads to a failure to meet the demand, causing an imbalance between the electric and mechanical torque, and consequently a sudden increase in the generator's speed, as Fig. 15 shows. In response to this increase, the pitch angle control acts, increasing the pitch angle to reduce the mechanical power in the turbine preventing speeds above its physical limits, this can be seen in Fig. 16. The inverse relationship between mechanical torque and the pitch angle is illustrated in Fig. 17.
In Fig. 13 it is possible to observe the operation of the reactive power control (VARFLAG = 1), responsible for the increase of the reactive power to compensate the voltage drop.
At t = 1.15 [s], the fault is cleared and the terminal voltage rises again. Because VLTFLG = 1, the voltage regulator will ensure

that the terminal voltage is adjusted to values close to the pre-fault situation.
At the end of the simulation, t = 20 [s], the system is already in steady state, with a slight decrease in the terminal voltage, which is expected, accompanied by an increase in the reactive power to compensate the removal of the defective line.

*O. VARFLG = 0 and VLTFLG =1*
The results for this simulation are presented below:

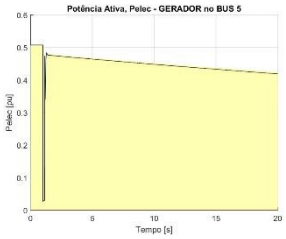


Fig. 19 - $P_{elec}$

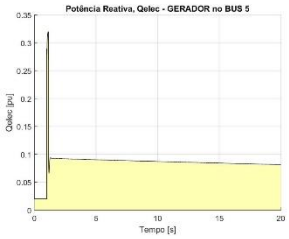


Fig. 20 - $Q_{elec}$

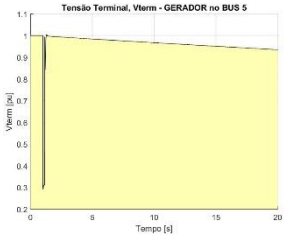


Fig. 21 - $V_{term}$

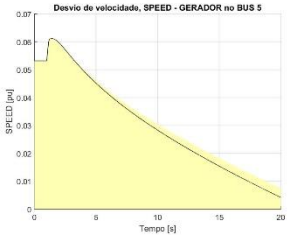


Fig. 22 - $SPEED$

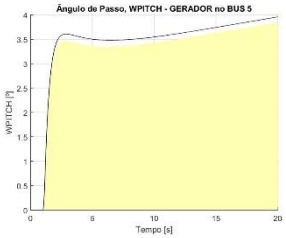


Fig. 23 - $WPITCH$

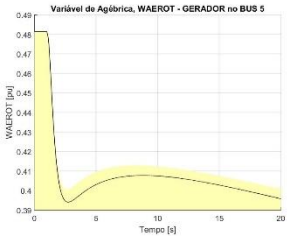


Fig. 24 - $WAEROT$

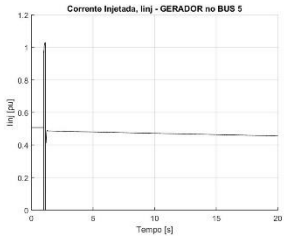


Fig. 25 – Injected Current

Before the fault, the system is again in steady state, as can be seen from the figures above. This confirms that the initial conditions are correct. When the fault occurs, the generator's terminal voltage drops, once again, to near zero, as shown in Fig. 21, due to the presence of the low impedance characteristic of a short circuit. Consequently, there is a sudden increase in the injected current by the generator in the network, as shown in Fig. 25.
The active power, again presents a similar behavior to the terminal voltage, as is verified in Fig. 19. This decrease in the active power leads to a failure to meet the demand, causing an imbalance between the electric and mechanical torque, and consequently a sudden increase in the generator's speed, as Fig. 22 shows. In response to this increase, the pitch angle control acts increasing the pitch angle to reduce the mechanical power in the turbine preventing speeds above its physical limits, this can be seen in Fig. 23. The inverse relationship between mechanical torque and the pitch angle is illustrated in Fig. 24.
At t = 1.15 [s], the fault is cleared and the terminal voltage increases. From this point on, the behavior of the model differs significantly from the case presented before.
With VARFLG = 0, the objective would be to keep the reactive power constant, which does not happen as shown in Fig. 20. Also Fig. 19, Fig. 21 and Fig. 25, show that the active power, the generator's terminal voltage and the current injected by the generator in the network do not stabilize, giving place to the conclusion that the stability of the system is not assured when this control mode is active.
Once again, it is possible to observe the operation of the voltage regulator, VLTFLG = 1, because the evolution of the terminal voltage and the active power, although not stabilizing, does not present significant overshoots.

*P. VARFLG = -1 and VLTFLG =0*
The results for this simulation are presented below:

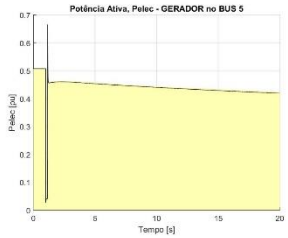


Fig. 26 - $P_{elec}$

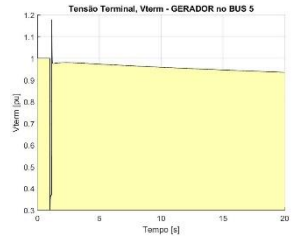


Fig. 27 - $V_{term}$

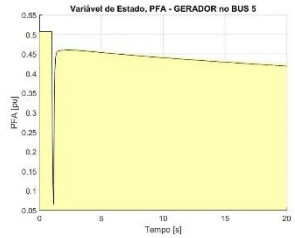


Fig. 28 - $PFA$

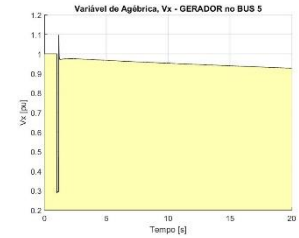


Fig. 29 - $V_X$

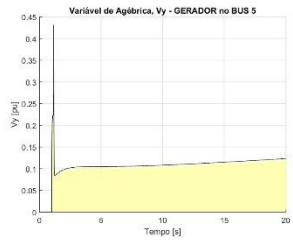


Fig. 30 - $V_Y$

This case, with VARFLG = -1, presents very similar behavior to the previous case. It is only presented in this paper to demonstrate the effects of not including the voltage regulator, VLTFLG = 0.

When bypassing this regulator, the difference between $V_r$ and $V_{term}$ will not be integrated to obtain the command for the internal voltage of the generator, WEQCMD, this will be obtained directly from the voltage $V_r$. Therefore, the generator's terminal voltage, $V_{term}$, will not be controlled, allowing its transient values to reach a considerable overshoot, as shown in Fig. 27. This overshoot has repercussions as well and as expected, on the generator's active power and on the algebraic

variables $V_X$ and $V_Y$ which represent the terminal voltage in the generator's reference frame, as can be seen in the Fig. 26, Fig. 29 and Fig. 30.

With VARFLG = -1, the objective would be to keep the power factor constant, but this does not happen, once again, as shown in Fig. 28. All the figures above also show that the stability of the system is not assured when this control mode is active.

## VI. Conclusions

This work focused on the implementation of generic WT3 models for transient stability studies of wind generators in a software for dynamic simulations of electric power systems that has been developed by students of I.S.T. using MATLAB.

First, it was necessary to understand the operation of the software. Second, the generic WT3 model under study was analyzed and then implemented. An effort was made not to change the software's structure to ensure that the models previously implemented would remain functional in this new version.

The dynamic models describing the generic WT3 model were taken from the model library of version 34 of the PSS/E™ software. A brief description of the models was made including some changes in the original models, due to some results not being satisfactory after the implementation. Alongside this description, the differential equations that represent the model were also presented.

This step deserved special attention because it is from this set of equations, which describe the transient behavior of WTGs, that the model is constructed in its algebraic form in order to allow for the implementation of the modified Euler-Cauchy integration algorithm. Any inaccuracies at this stage would result in serious implementation errors and the non-validation of the models under study.

Finally, the results of the simulations performed were presented and analyzed, concluding that the implemented models fulfilled the primary objective of representing realistically the WT3 generic model. To reach this conclusion, the results were validated against results obtained with the PSS/E™ software, each incoherence was treated and solved and several implementation errors were rectified.

## APPENDIX A

Table A.1 – Default Parameters values

| ***Parameter*** | ***Default Value*** |
|---|---|
| $\omega p_{min}$ | 0.69 pu |
| $\omega p_{20}$ | 0.78 pu |
| $\omega p_{40}$ | 0.98 pu |
| $\omega p_{60}$ | 1.12 pu |
| $P_{\omega p_{100}}$ | 0.74 pu |
| $\omega p100$ | 1.2 pu |

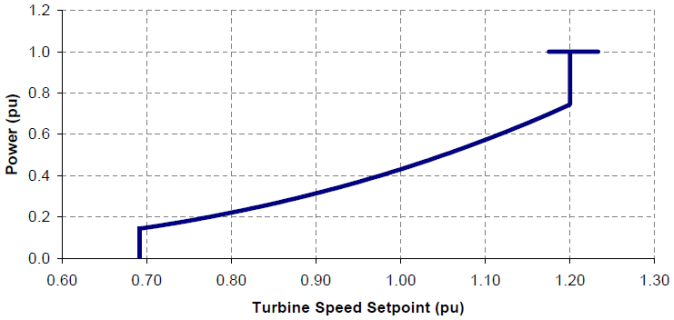


Fig. A.1 - Typical Power vs Speed characteristic

## References


Araújo, P. (2009). *Dynamic Simulations in Realistic-Size Networks.* (IST, Ed.) Lisboa, Portugal.

Cheng, X. (2015). *Employing Online Data for Dynamic Equivalent Model.* The University of Texas at Arlington: Tese de Doutoramento.

DGEG. (2016). *Renováveis - Estatisticas rápidas nº146 - Dezembro 2016.* Direcção Geral de Energia e Geologia. Retrieved from http://www.dgeg.gov.pt?cr=15736

Ferreira de Jesus , J., & Castro, R. (2004). *Equipamento Eléctrico dos GeradoreS - 1ª Parte – Princípio de Funcionamento.*

Lacerda, A. (2013). *Modelos de FACTS para Estudos de Estabilidade Transitória.* Lisboa: Tese de Mestrado, Instituto Superior Técnico.

Milano, F. (2010). *Power System Modelling and Scripting.* London: Springer.

Paulo, A. (2008). *A Library of Dynamic Models for Transient Stability.* (IST, Ed.) Lisboa, Portugal.

PSS/E. (2006). *Generic Type-3 Wind Turbine-Generator Model for Grid Studies.* (PSS/E, Ed.) New York.

REN. (2016). *Dados Técnicos 2016 - Electricidade.* Retrieved from http://www.centrodeinformacao.ren.pt/PT/InformacaoTecnica/DadosTecnicos/REN%20Dados%20T%C3%A9cnicos%202016.pdf

Siemens. (2015). *PSS/E 34.0 Model Library.*

Sucena Paiva, J. P. (2005). *Redes de Energia Eléctrica: Uma Análise Sistémica.* Lisboa: IST Press.

Yuriy, K., & Krishnat, P. (2009). *PSS®E Generic WT3 Wind Model - User Guide.* Siemens Energy, Inc.